

CURVED FIBER SCATTERING

S. Alyones [†]

Physics Department
The Hashemite University, Zarqa 13115, Jordan

C. W. Bruce

Physics Department
New Mexico State University, Las Cruces, NM 88001, USA

Abstract—Extinction and backscattering from thin curved fibers of finite conductivity are computed by solving the Pocklington integro-differential equation using the Moment Method with point matching scheme. For simplicity of interpretation these computations were performed at long wavelengths, in the Drude domain. The effect of the degree of curvature on the cross sections is examined for high and low fiber conductivities, and for two incident geometries: normal and parallel to the plane of the curved fiber. The computations show a narrowing and decreasing cross sections with increased fiber curvature for both low and high conductivities. The normal geometry produces larger cross sections than the parallel case.

1. INTRODUCTION

The subject of electromagnetic scattering by small particles has been under investigation for a number of decades with recent developments in both particles and theory [1]. The electromagnetic scattering and absorption of a small particle depends on the size, shape and the material content (as found in the complex dielectric function) of the particle. Communications, atmospheric imagery, environmental (radiative transfer) and astronomical interests, among others, are involved.

Received 10 January 2011, Accepted 25 March 2011, Scheduled 29 March 2011

Corresponding author: Sharhabeel Alyones (salyones@hu.edu.jo).

[†] S. Alyones is also with Physics Department, New Mexico State University, Las Cruces, NM 88001, USA.

Straight, thin, finite conducting fibrous particles have also long been used for electromagnetic shielding, both in airborne and in solid matrices. In the last few years [2–6] the theory for this form of particle has been solidified and confirmed in a number of publications, from short wavelengths to the microwave. One of these theories [2] also applies when the fibers have a finite diameter ($kD/2 < 1$), where k is the free space wave number and D is the diameter of the fiber, although the extent of the aspect ratio L/D (for small values) is somewhat circumscribed, where L is the fiber length. Here we are concerned with the effects of fiber curvature on the effective cross sections.

To a very good approximation, the electromagnetic scattering and absorption of finite conducting straight thin fibers are described by the Pocklington integro-differential equation. Both analytical and numerical solutions have been obtained and verified by means of measurements and theoretical comparisons [2–11]. To study the effect of fiber curvature on electromagnetic scattering, we present a numerical solution for the Pocklington integro-differential equation that describes the curved fiber scattering. The moment method of reference [2] with point matching scheme (using short range pulse basis functions) is used to obtain the solution. The fiber has been modeled as a half arc ellipse wherein the eccentricity of the ellipse is changed from 1 (straight fiber) to 0 (half circle) to illustrate the spectrum of responses. Also, the problem is solved for two polarizations of incident orientation: In the first case the incident plane electromagnetic wave encounters the fiber with the k -vector directed parallel to the plane of the fiber, and in the second case the electromagnetic wave hits the fiber with direction normal to the fiber plane.

The computations reported here for long wavelengths can be scaled to short wavelengths (IR and Visible), providing that the dispersion theory is used for the dielectric function of the fiber material. Even though the same computational technique in [2] is used here, the computations for curved fibers reported here are important for those dealing with micro and nano fibers, which mostly tends to be curved rather than straight as the diameter becomes smaller, and those fibers include artificial and air born fiber like particles in the atmosphere. This is particularly relevant as man-made fiber diameters decrease and become more flexible.

2. FORMULATION OF THE PROBLEM AND THE MOMENT METHOD

Consider a curved elliptical thin conducting fiber with eccentricity (ϵ), Diameter (D), length (L), conductivity σ , relative magnetic

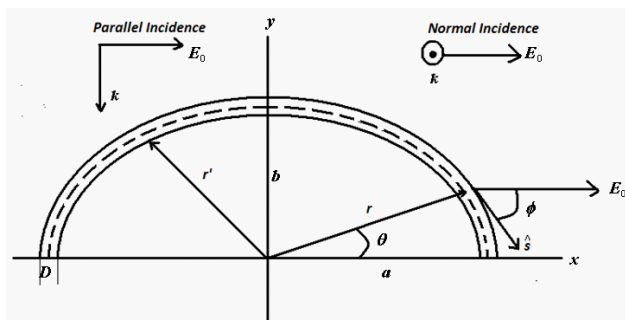


Figure 1. Geometry for a plane wave impinging a curved fiber.

permittivity μ_r , and relative dielectric constant ϵ_r lying in the x - y plane as shown in Figure 1. When a plane electromagnetic wave (with time dependent $e^{-i\omega t}$) impinges the fiber, assuming that the aspect ratio $L/D \gg 1$ and $kD/2 < 1$, the dimensionless induced surface current $u(\vec{r})$ is determined by the Pocklington integro-differential equation [2–5]:

$$\hat{s} \cdot \vec{E}_0 e^{i \vec{k} \cdot \vec{r}} = \int_l ds' u(\vec{r}') \left(\hat{s} \cdot \hat{s}' - \frac{1}{k^2} \frac{\partial^2}{\partial s \partial s'} \right) G(\vec{r}, \vec{r}') - \eta u(\vec{r}) \quad (1)$$

where $R = |\vec{r} - \vec{r}'|$, $G(\vec{r}, \vec{r}') = \frac{e^{ikR}}{R}$ is the free space Green's function and \hat{s} is the tangent to the fiber at the field point. To avoid the singularity in the Green's function during the calculations of the matrix elements in the Moment method, the source point \vec{r}' is always assumed to be on the wire surface, while the field point \vec{r} is on the wire axis, as shown in Figure 1. η is the dimensionless surface impedance which is defined in terms of the first two Bessel functions and the bulk parameters of the fiber material [5].

The equation of an ellipse, with major axis a and minor axis b , in Cartesian and polar coordinates for an origin at the center of the ellipse is given by, respectively:

$$r(\theta) = \frac{ab}{\sqrt{(b \cdot \cos(\theta))^2 + (a \cdot \sin(\theta))^2}} \quad (2)$$

$$\frac{x^2}{a^2} + \frac{y^2}{b^2} = 1 \quad (3)$$

From these two equations, the tangential angle φ is related to the polar angle θ through the relation:

$$\tan(\varphi) = -\frac{b^2}{a^2} \cot(\theta) \quad (4)$$

Also the eccentricity and an element of length of an ellipse are given by:

$$\epsilon = \sqrt{1 - \left(\frac{b}{a}\right)^2}, \quad ds = \sqrt{(r(\theta))^2 + \left(\frac{dr(\theta)}{d\theta}\right)^2} \cdot d\theta \quad (5)$$

If Equations (2)–(5) are implemented in the Pocklington Equation (1), Equation (1) will have the following form in terms of the polar angle (θ) for normal and parallel incidence geometries, respectively:

$$\cos(\phi) \left\{ E_0 e^{-ikr \sin(\theta)} = \int_{\pi}^0 d\theta' u(\vec{r}') \left(\cos(\theta - \theta') - \frac{1}{k^2 \cdot \sqrt{(r(\theta))^2 + \left(\frac{dr(\theta)}{d\theta}\right)^2}} \frac{\partial^2}{\partial\theta\partial\theta'} \right) G(\vec{r}, \vec{r}') - \eta u(\vec{r}) \right\} \quad (6)$$

The Moment method of reference [2] will be used to solve Equation (6) for both incidence cases. For the computation using the Moment method, the fiber length is divided into N intervals (number of matching points), and the current is expanded in terms of a short range pulse basis function over the fiber length. Then we assert that the Pocklington equation be satisfied at the center of each interval. This converts the Pocklington equation into a system of linear equations whose solution is the current over the fiber. Once we have the current in hand, one can easily obtain the scattering, absorption, backscattering, and extinction (absorption + scattering) cross sections from the far field amplitude [2–5]. The number of intervals N , is doubled until convergence is achieved over the cross sections.

3. RESULTS AND DISCUSSION

Fortran codes were written based on the Moment Method to solve the system of Equation (6), and extensive computations were performed with convergence achieved for both cases of incident geometries with in an error less than 0.001. The computational CPU times are comparable with those reported in reference (2) for straight fibers. Figures 2 and 3 show an example of the convergence of the extinction cross section for a lowly conductive curved fiber as the number of matching points (number of basis functions) N increases for the two incidence geometries. As a validation of the computational model, the solution obtained satisfies the boundary condition that the current vanishes at the end points of the fiber as seen in the examples below.

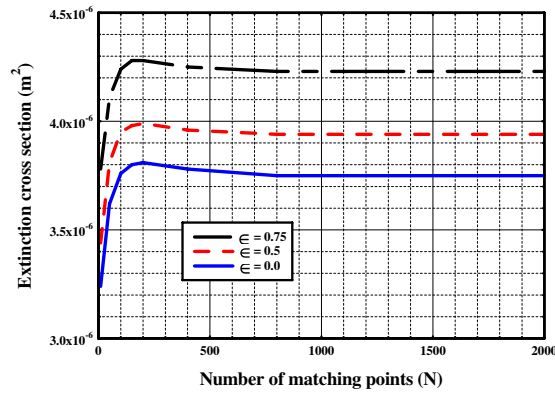


Figure 2. Extinction cross section versus number of matching points N for a lowly conductive fiber of total length 6 mm, diameter $8\ \mu\text{m}$, conductivity 7×10^4 mho/m at frequency 35 GHz for normal incidence geometry.

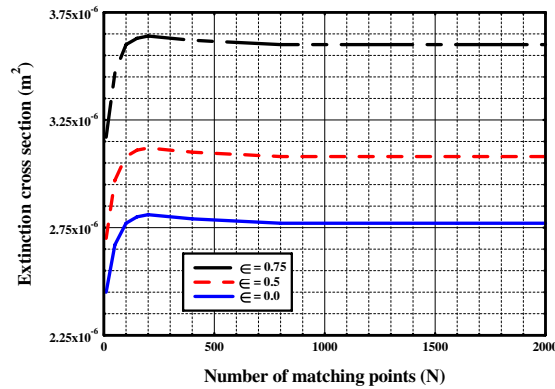


Figure 3. Extinction cross section versus number of matching points N for a lowly conductive fiber of total length 6 mm, diameter $8\ \mu\text{m}$, conductivity 7×10^4 mho/m at frequency 35 GHz for parallel incidence geometry.

Another test of the computational model is that the solution should satisfy the energy balance condition: the extinction cross section, when calculated from the forward scattering amplitude, should equal the addition of the scattering and absorption cross sections [2, 5]. Table 1 shows calculations for various cross sections for a highly conductive curved fiber for the two incidence geometries; the table shows that energy balance condition is perfectly met. Also, in both

Table 1. Calculations of various cross sections for a highly conductive curved fiber of total length 4 mm, diameter 8 μm , conductivity 6×10^7 mho/m at frequency 35 GHz.

Cross Section $\times 10^{-5} \text{ m}^2$	Normal incidence ($\epsilon = 0.0$)	Normal incidence ($\epsilon = 0.5$)	Normal incidence ($\epsilon = 0.75$)	Normal incidence ($\epsilon = 0.0$)	Normal incidence ($\epsilon = 0.5$)	Normal incidence ($\epsilon = 0.75$)
Extinction	3.260	3.330	3.380	2.460	2.650	2.920
Scattering	3.051	3.122	3.176	2.257	2.448	2.720
Absorption	0.209	0.208	0.204	0.203	0.202	0.200
Scattering + Absorption	3.260	3.330	3.380	2.460	2.650	2.920

cases of incidence geometries, as the curvature decreases the cross section solution converges to the straight wire solution as seen in the examples below, another evidence of the accuracy of the solution. It should be mentioned here that another computational approach and experimental data are needed to verify the results reported here.

The results that follow are for incident plane waves, frequency of 35 GHz and a fiber of (4 μm) diameter. The objective is to use these parameters to compare cross sections for straight fibers and several degrees of fiber curvature, for both incident geometries, and for low and high conductivities.

3.1. High Conductivity Fibers

Figures 4 and 5 show the extinction and backscattering cross sections as a function of fiber length, for a conductivity of 6×10^7 mho/m (close to that of silver, copper and aluminum). The range of lengths includes the first resonance length region for scattering by a straight fiber.

Figures 4 and 5 show that, for normal incidence geometry, as the fiber curvature increases, the cross sections (extinction and backscatter) both become narrower compared with the straight fiber response. Also there is a slight shift of the resonance peak.

Figures 6 and 7 show the extinction and backscattering cross sections for the same parameters of Figures 4 and 5 but for parallel incidence geometry. These figures show that as a fiber becomes progressively more curved the cross section decreases and becomes narrower with the same slight resonant shift.

In order to understand this behavior, the induced current is plotted for the fiber lengths: 4.1 mm (peak length), 6 mm (off peak

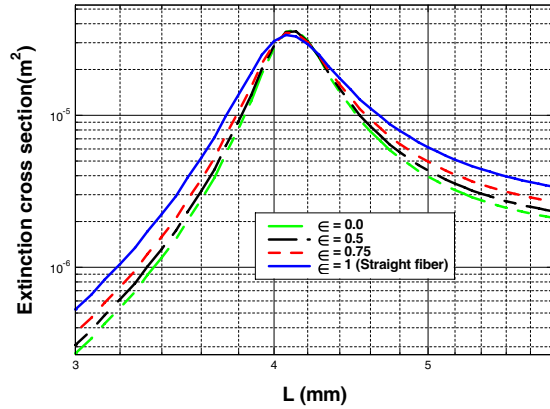


Figure 4. Extinction cross section versus fiber length at 35 GHz incident plane wave for normal incidence geometry, $D = 4 \mu\text{m}$, $\sigma = 6 \cdot 10^7 \text{ mho/m}$.

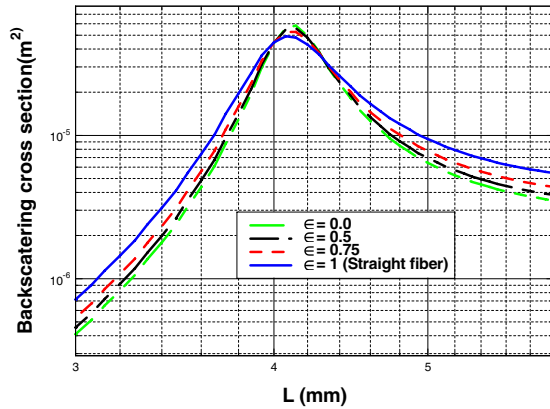


Figure 5. Backscattering cross section versus fiber length at 35 GHz incident plane wave for normal incidence geometry, $D = 4 \mu\text{m}$, $\sigma = 6 \cdot 10^7 \text{ mho/m}$.

length), for $\epsilon = 0.5$, and for both incident geometries. Figures 8 and 9 show these current plots as a function of the polar angle (θ).

From these figures, we see that:

- 1) For the resonant length the current becomes more peaked toward the fiber center as the fiber curvature increases, with the value at the center of the fiber slightly higher for normal geometry than for parallel geometry. For the off peak length, the currents are all considerably lower. The curved fibers are still more peaked

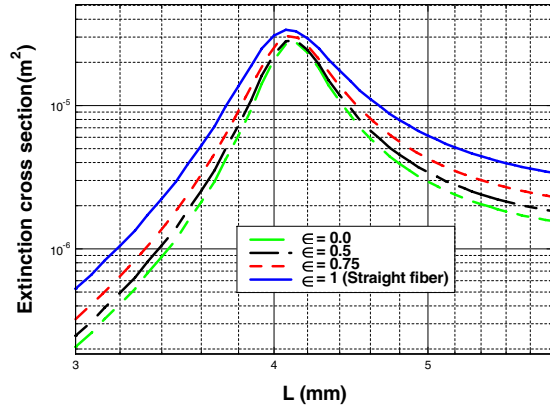


Figure 6. Extinction cross section versus fiber length at 35 GHz incident plane wave for parallel incidence geometry, $D = 4 \mu\text{m}$, $\sigma = 6 \cdot 10^7 \text{ mho/m}$.

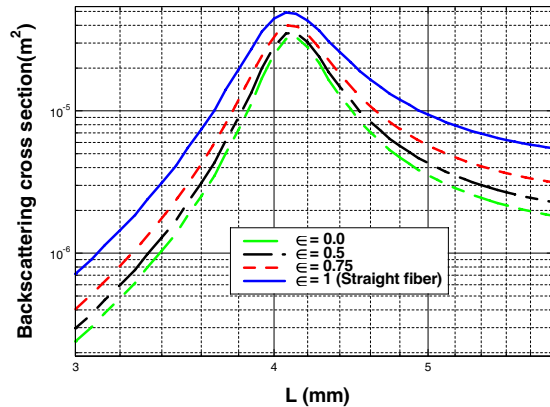


Figure 7. Backscattering cross section versus fiber length at 35 GHz incident plane wave for parallel incidence geometry, $D = 4 \mu\text{m}$, $\sigma = 6 \cdot 10^7 \text{ mho/m}$.

than that for the straight fiber but less so and with lower relative amplitude at the center of the fiber for both cases of incident geometries.

- 2) The resonance shift might be explained by saying that, for the curved fibers, the apparent projected fiber length decreases. Notice that for normal incident geometry, the entire fiber is excited in phase. That excitation in the parallel geometry is not in phase might suggest the source of the lower cross sections for this case.

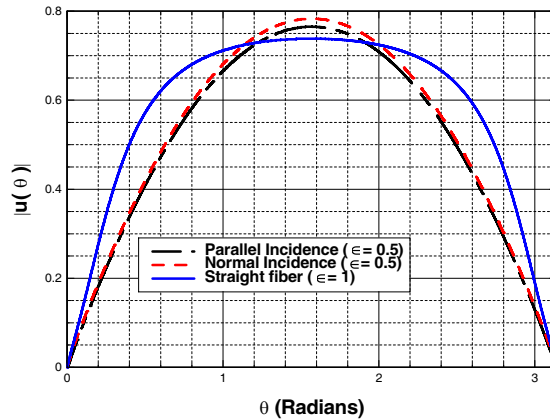


Figure 8. Amplitude of induced surface current versus polar angle at 35 GHz incident plane wave, at the straight wire first resonant peak length $L = 4.1$ mm, $D = 4$ μm , $\sigma = 6 \cdot 10^7$ mho/m.

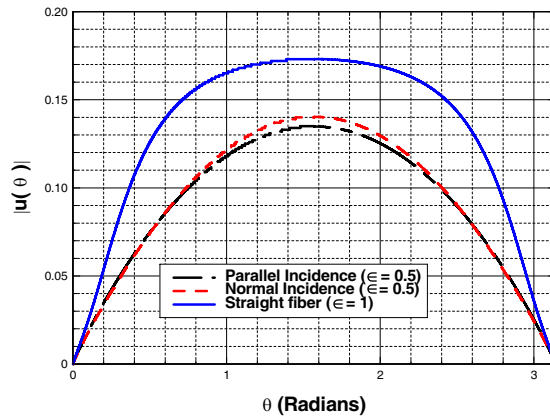


Figure 9. Amplitude of induced surface current versus polar angle at 35 GHz incident plane wave, at an off peak length $L = 6$ mm, $D = 4$ μm , $\sigma = 6 \cdot 10^7$ mho/m.

3.2. Low Conductivity Fibers

Figures 10 and 11 show the extinction for fibers with a conductivity of $\sigma = 7 \times 10^4$ mho/m, (graphite like conductivity). It is well known that low conductivity fibers are essentially not resonant and so, for curved, low conductivity fibers in the Drude, low wavelength domain, cross sections simply decrease as expected with no appearance of resonance.

Figure 12 shows the corresponding current at 4.1 mm length fiber. One can see that the current reduced, so the efficiency is reduced for fiber curvature for both cases of incident geometry. Again the normal geometry is more efficient than the parallel geometry due to the same reason (reduced excitation efficiency).

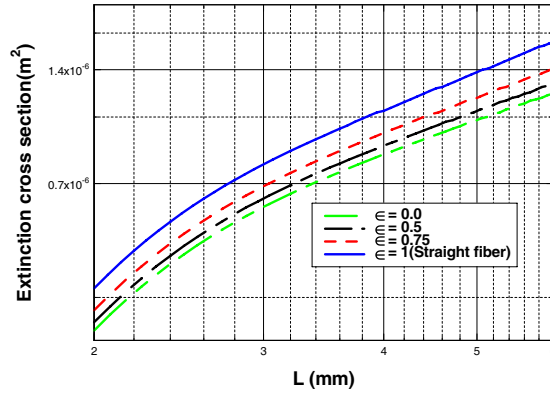


Figure 10. Extinction cross section versus fiber length at 35 GHz incident plane wave for normal incidence geometry, $D = 4 \mu\text{m}$, $\sigma = 7 \cdot 10^4$ mho/m.

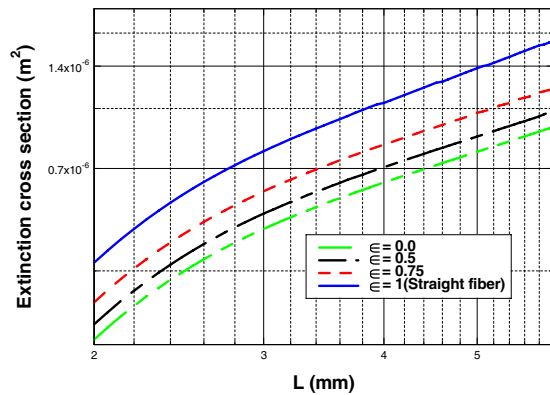


Figure 11. Extinction cross section versus fiber length at 35 GHz incident plane wave for parallel incidence geometry, $D = 4 \mu\text{m}$, $\sigma = 7 \cdot 10^4$ mho/m.

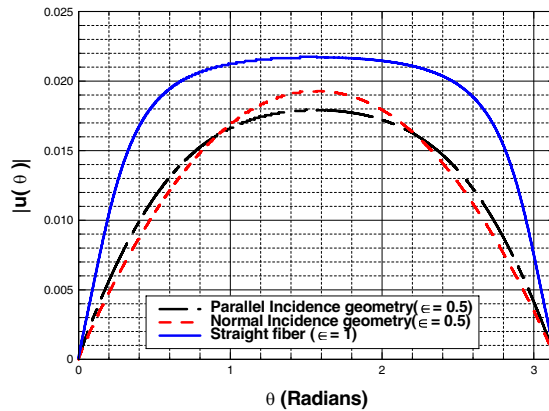


Figure 12. Amplitude of induced surface current versus polar angle at 35 GHz incident plane wave, fiber length $L = 4.1$ mm, $D = 4$ μm , $\sigma = 7 \cdot 10^4$ mho/m.

4. CONCLUSION

The problem of electromagnetic scattering by finite conducting thin curved fiber has been solved numerically using the moment method with point matching scheme. The problem has been solved for two different geometries to indicate the effect of fiber curvature on its response to electromagnetic radiation. Characterizing the effect of curvature to the electromagnetic response is relevant to those having an interest in attenuation efficiencies of very thin fibers. It has been shown in this paper that curvature of the fiber reduces its response except at the resonance peak length for the normal geometry while the parallel case experiences a reduction in response due the variable phase excitation along the fiber, with a slight resonance shift for both cases.

ACKNOWLEDGMENT

Our many thanks go to Mr. Jeff Hale of the Edgewood Chemical and Biological Center, U.S. Army for his support of this research through contract DAAD13-03-D-0012 with Science and Technology Corp.

REFERENCES

1. Mishchenko, M. I., L. D. Travis, and A. A. Iacis, *Scattering, Absorption, and Emission of Light by Small Particles*, Third

- electronic release, NASA Goddard Institute for Space Studies, New York.
2. Alyones, S., C. W. Bruce, and A. Buin, "Numerical methods for solving the problem of electromagnetic scattering by a finite thin conducting wire," *IEEE Trans. Antennas and Propagation*, Vol. 55, No. 6. Jun. 2007.
 3. Waterman, P. C., "Scattering, absorption, and extinction by thin fibers," *J. Opt. Soc. Am. A*, Vol. 22, No. 11, Nov. 2005.
 4. Waterman, P. C. and J. C. Pederson, "Electromagnetic scattering and absorption by finite wires," *J. Appl. Phys.*, Vol. 78, 656–667, 1995.
 5. Waterman, P. C. and J. C. Pederson, "Scattering by finite wires of arbitrary ϵ , μ , σ ," *J. Opt. Soc. Am.*, Vol. 15, 174–184, 1998.
 6. Burke, G. J., *Numerical Electromagnetic Code (NEC)-Method of Moment; Part I: Program Description-Theory, Part II: Program Description-Code, Part III: User's Guide*, Rep. UCID-18834, Lawrence Livermore Nat. Lab., Livermore, CA, Jan. 1981.
 7. Bruce, C. W., A. V. Jelinek, S. Wu, S. Alyones, and Q. Wang, "Millimeter wavelength investigation of fibrous aerosol absorption and scattering properties," *Appl. Opt.*, Vol. 43, Dec. 20, 2004.
 8. Bruce, C. W. and S. Alyones, "Extinction efficiencies for metallic fibers in the infrared," *Appl. Opt.*, Vol. 48, 5095–5098, Sep. 20, 2009.
 9. Jelinek, A. V. and C. W. Bruce, "Extinction spectra of high conductivity fibrous aerosols," *J. Appl. Phys.*, Vol. 78, 2675, 1995.
 10. Gurton, K. P. and C. W. Bruce, "Parametric study of the absorption cross section for a moderately conducting thin cylinder," *Appl. Opt.*, Vol. 34, 2822, 1995.
 11. Alyones, S. and C. W. Bruce, "Electromagnetic scattering by finite conducting fiber: Limitation of a previous published code," *Journal of Electromagnetic Waves and Applications*, Vol. 25, No. 7, 1021–1030, 2011.